

# Spectral Reflectance Response of Big Sagebrush to Hydrocarbon-Induced Stress in the Bighorn Basin, Wyoming\*

Bobby H. Bammel and Richard W. Birnie

## Abstract

A geobotanical reflectance study was conducted at five areas in the Bighorn Basin of Wyoming to determine if the spectral responses of sagebrush could be a useful tool in hydrocarbon exploration. Measurements were collected in the visible and near infrared regions (0.45 to 1.1  $\mu\text{m}$ ).

This investigation shows that a consistent and significant blue shift (to shorter wavelengths) of the green peak (0.56  $\mu\text{m}$ ) and red trough (0.67  $\mu\text{m}$ ) positions is the most reliable indicator of hydrocarbon-induced stress in sagebrush plants. This shift can only be detected where the sage is actually growing in large amounts of surface-visible or near-surface hydrocarbons. Spectral reflectance intensity data were found to have no significant correlation with the presence or absence of surface or subsurface hydrocarbons.

## Introduction

This study was undertaken to determine the usefulness of the spectral response of sagebrush (*Artemisia tridentata*) as a possible tool in commercial hydrocarbon exploration. Reflectance spectra were measured and analyzed from over 450 sagebrush plants from 150 locations in the Bighorn Basin, Wyoming (Figure 1). Sites were selected over and around producing oil and gas fields, and at two surface hydrocarbon deposits. Anomalously high vertical hydrocarbon microseepage from underlying petroleum reservoirs could cause surface and near-surface geochemical changes in the soils which would in turn promote geobotanical alteration. Vertical movement is greatly enhanced by faults, fractures, and microfractures.

In some areas vertically seeping hydrocarbons have caused changes in the surface and near-surface mineralogy of the bedrock and geochemistry of the soils (Donovan, 1974; Malhotra, 1988; Segal and Merin, 1989). Visible changes may include bleaching of iron-oxide rich formations, induration by calcium carbonate, and alteration of gypsum to calcite (Crawford, 1991).

High resolution portable spectrometers are able to discriminate subtle variations in vegetation pigment absorption and reflectance characteristics throughout wide spectral regions and with a quantitative precision not possible with the human eye. Numerous multispectral geobotanical reflectance

studies have shown a good correlation between anomalous vegetation responses and the location of subcropping mineralized zones (Goetz *et al.*, 1983; Birnie and Francica, 1981; Singhroy and Kruse, 1991). Although most of these studies have been concerned with mineral exploration, several recent works have dealt with hydrocarbon exploration (Malhotra, 1988; McCoy *et al.*, 1989).

## Sample Areas

The Little Buffalo Basin, Bonanza, and Enigma fields are all located along the "basin margin anticlinal" trend (Fox and Dolton, 1989) of the Bighorn Basin. Production in the Little Buffalo Basin Field is distributed in a bidomal accumulation with shallow gas found only at the east dome. A separate analysis was also performed using only the east dome data as a sixth sample area. All three of these fields were actively producing hydrocarbons in 1990 and 1991 (Figure 1 and Table 1).

The Trapper Canyon Tar Sand Deposit is a surface tar sand occurrence located on the western flank of the Bighorn Mountains. Several drill holes and outcrop sections indicate that the tar impregnated sand measures about 3 metres in thickness. The Trapper Canyon deposit is unique when compared against the other three producing oil and gas fields in several respects; these include (1) a higher elevation, (2) different sagebrush subspecies, (3) hydrocarbon deposit is found at surface only, and (4) different outcropping surface formations.

The Cody Base Deposit is located in Washakie County, Wyoming, about 2 to 4 kilometres south and south-southeast of the Enigma Field in an area known *not* to contain surface or subsurface hydrocarbons. Several dry holes drilled in the area resulted from an effort to find commercial hydrocarbons here; a subtle structural high can be mapped using the well control provided by the dry holes. Samples were taken from representative sages in the exact same manner as at the producing fields. A completely fictitious and arbitrary field boundary, center, and axis were sketched on the sampled area, and used for statistical analysis as explained later.

\*Presented at the Ninth Thematic Conference on Geologic Remote Sensing, Pasadena, California, 8-11 February 1993.

Department of Earth Sciences, Dartmouth College, Hanover, NH 03755. B.H. Bammel's present address is Hardin-Simmons University, Abilene, TX 79698.

Photogrammetric Engineering & Remote Sensing, Vol. 60, No. 1, January 1994, pp. 87-96.

0099-1112/94/6001-87\$03.00/0  
©1994 American Society for Photogrammetry and Remote Sensing

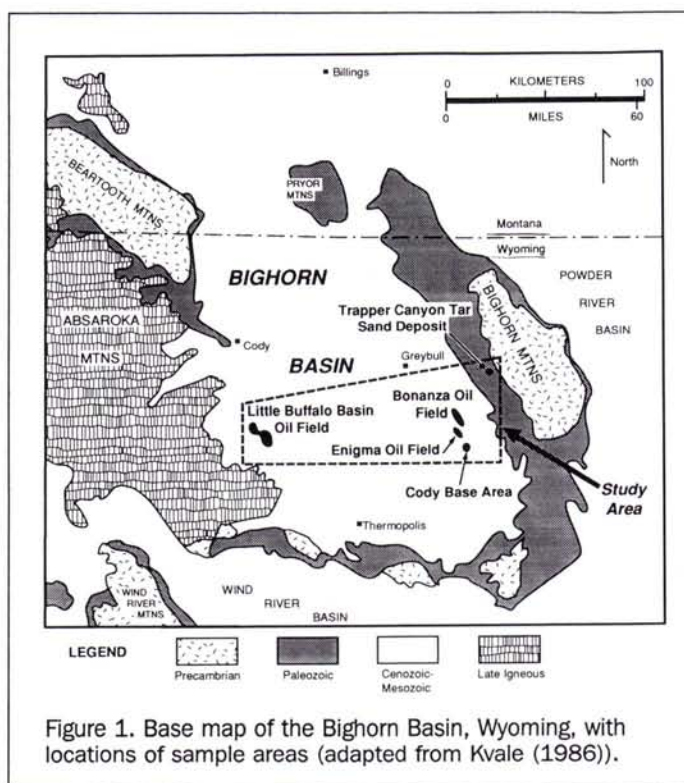


Figure 1. Base map of the Bighorn Basin, Wyoming, with locations of sample areas (adapted from Kvale (1986)).

The four hydrocarbon-bearing areas were specifically chosen in order to test for the effects of microseepage on contrasting reservoir types and production depths. Within these four areas are found shallow gas (Little Buffalo Basin), intermediate-depth oil (Bonanza), moderately deep oil (Little Buffalo Basin and Enigma), highly viscous "dead oil" (Trapper Canyon), and an active oil and gas oil seep (Bonanza). In a broad sense, the areas chosen for study can be divided into three distinct area-types: (1) "extreme" examples where hydrocarbons can be observed at the surface as tar or hydrocarbon seeps (Trapper Canyon and Bonanza Seeps), (2) areas devoid of surface and subsurface hydrocarbons (Cody Base), and (3) "intermediate" sites at which subsurface hydrocarbons are present and actively produced (Little Buffalo Basin, Bonanza, and Enigma).

## Hydrocarbon Microseepage

Extensive evidence in favor of vertical migration of hydrocarbon gases from subsurface petroleum reservoirs has been presented during the past 30 years, including remote sensing methods (Lang *et al.*, 1984; Malhotra, 1988; McCoy *et al.*, 1989), biogeochemistry (Dalziel and Donovan, 1980; Mitchell, 1988; McCoy *et al.*, 1988; Klusman *et al.*, 1992), and stable isotopes (Donovan, 1974; Oehler and Sternberg, 1984). This movement is greatly enhanced by faults, fractures, and microfractures, and can change the surface and near-surface mineralogy of the bedrock, geochemistry of the soils, and vegetational reflectance. In structural traps, such as Little Buffalo Basin, Enigma, and Bonanza, the highest density of fractures, microfractures, and hydrocarbons would be anticipated along the crest of the fold due to maximum deformation.

As hydrocarbons seep upward toward the surface, they encounter oxygenated pore fluids and may be attacked and consumed by aerobic bacteria (Dalziel and Donovan, 1980). Work by Klusman *et al.* (1992) concludes that oxidation of seeping hydrocarbons causes an increase in uptake by the plants of transition trace elements such as iron, manganese, and vanadium, and a decrease in uptake of alkaline earth elements such as calcium, strontium, and barium.

## Wyoming Big Sagebrush

Within the study area, the big sagebrush or sage (*Artemisia tridentata* vars. *tridentata*, *wyomingensis*, and *vaseyana*) are among the most widespread vegetation found. Due to its ubiquity and existing works dealing with sage's response to hydrocarbon microseepage, *Artemisia tridentata* were systematically sampled over the five areas of interest.

Four of the study areas (Bonanza, Little Buffalo, Enigma, and Cody Base) are located well within the basin at relatively low elevations of less than 1900 metres, where only samples from Wyoming big sagebrush (var. *wyomingensis*) were sampled. At the Trapper Canyon Tar Sand Deposit, elevation 2250 metres on the southwest flank of the Bighorn Mountains, only *Artemisia tridentata* var. *vaseyana*, commonly known as Mountain big sagebrush, is found. All samples at the Trapper Canyon area were made on Mountain big sagebrush.

## Methods

Hand-held high resolution spectral reflectance data were gathered from sagebrush at five different areas in the Bighorn Basin during two field seasons, September and early October, 1990 and August and September, 1991.

The Spectron Engineering SE590 Data-Logging Spectro-

TABLE 1. PRODUCTION STATUS AND GEOLOGY OF AREAS OF INTEREST

Sample Area	Status	Surface Structure & Geology	Remarks
Little Buffalo Basin Field	producing oil and gas	anticline Cody Shale at surface	oil from >1260m (Phosphoria & Tensleep) gas from 366m, 615m, 690m (Frontier, Muddy, & Cloverly formations)
Bonanza Field	producing oil & active seep	anticline Mowry Shale at surface	oil from 750 m (Tensleep Fm.) active oil/gas seep at surface (Mowry Sh.)
Enigma Field	producing oil	No surface structure Cody Shale at surface	oil from 1320m (Tensleep Fm.)
Trapper Canyon Tar Sand	tar sand outcrop	No surface structure Tensleep Ss. at surface	surface outcropping tar sands (Tensleep Ss.)
Cody Base	no oil or gas	No surface structure Cody Shale at surface	sample area with no production

radiometer/Spectrometer was used to make all of the measurements. The spectral bandwidths range from 0.0026 to 0.0032 micrometres and average about 0.0028 micrometres.

Several field guidelines were followed during acquisition of the data in order to maintain maximum consistency. Several of these guidelines are also discussed in McCoy *et al.* (1989).

- Three sagebrush plants were measured and averaged at each site. This was done to broaden the database and to compensate and/or dampen the effects of wind, shadows, or other anomalous features present on one plant.
- Work periods were limited to periods of high solar altitude, usually between 10:00 AM and 4:00 PM each day. This practice insured maximum foliage reflectance and minimum shadow effects.
- Reflectance from a reference panel was obtained at each site to standardize for changing solar illumination.
- The detector head was maintained in a constant position relative to the sun.
- Work was limited to cloud-free days or times during the day when clouds did not interfere with the sun's full illumination at the site.

### Field Spectral Measurements

At each sample site three kinds of spectral measurements were taken on each of three closely spaced sagebrush plants, consisting of (1) black cloth (BC), (2) clump (CL), and (3) fiber optic (FO) readings. A separate Fiberfrax reference panel measurement was made prior to the scanning of individual data sets. Fiberfrax is a synthetic crystalline silica product that is both highly reflective and diffusive with respect to electromagnetic radiation within the spectral region of interest.

In "black cloth" measurements the detector head was set up on a tripod about one metre away from the sage, with a black cloth ground skirt covering the underlying ground. At this distance reflected radiation from an area of about 10 centimetres in diameter was recorded. The skirt was intended to prevent spectral contamination from any underlying soils, rocks, debris, and other vegetation. In the black cloth readings an attempt was made to measure a representative portion of the plant. In general, most of the field of view would be composed of healthy leaves, but branches, shadows, and dead leaves might also be present depending on the individual plant. For each site the spectral measurements of all three plants were later ratioed against the same Fiberfrax standard reading and then averaged to arrive at the final black cloth percent reflectance spectrum for that particular site.

After the black cloth measurements were collected, branches from two of the sagebrush plants were cut and placed into open or sparse spots on the third plant. This was done in order to create a tight "clump" of vegetation incorporating all three plants, dominated by healthy sage leaves. Branches, shadows, and any other underlying contamination were, for the most part precluded from incorporation into this measurement. The detector head remained about 1 metre from this clump and, therefore, again incorporated an oval area measuring 10 centimetres in diameter. Three reflectance spectra were obtained from the clump, ratioed against the reference, and averaged.

Fiber optic measurements of individual leaves were obtained by employing a thin (approximately 1- to 2-mm diameter) clear filament. Use of this probe yielded a reading incorporating 100 percent typical foliage and allowed spectral readings of individual leaves. At least one leaf from each of the three sages was measured, and, generally, eight representative leaf readings (two or three from each plant) were taken and averaged from each site. The three types of spectral readings are intended to measure a wide range of reflectance

characteristics exhibited in the sagebrush. The black cloth reflectance measurements take into account not only the leaf reflectance but also a significant plant morphology component, including leaf density, shadowing, leaf orientation, and branching. The clump set incorporates significantly more foliage reflectance, and minimizes the plant morphology component. The fiber optic set completely eliminates the inclusion of any plant morphology aspect and only contains information relevant to leaf reflectance. Analyses of these three different data sets are intended to determine which spectral characteristic(s) of the plants are most relevant to the presence of hydrocarbons in the soil and to its potential use in subsurface hydrocarbon exploration.

### Data Processing of SE590 Spectra

The initial processing of the 252-channel raw data involved the removal of 47 spectral channels from each file. Reflectance values in the first 35 and last 12 spectral channels of the Fiberfrax reference panel produced unacceptable signal-to-noise ratios in the data, due to low source illumination in these spectral regions.

The trimmed spectral reflectance values extend in wavelength from 0.455 to 1.088 micrometres. These data were manipulated further in two ways. The remaining 205 spectral channels were averaged over five channels, producing a 41-channel spectrum with resulting bandwidths of approximately 0.015 micrometres. Adjacent spectral values in the original data are highly correlated, and, therefore, little information is lost due to this averaging technique. The new 41-channel data are intended to allow examination over the entire breadth of useful data acquired, and reduce signal-to-noise ratios in a small enough package for convenient and meaningful analysis.

A number of specific features from each spectrum were also extracted for analysis. These spectral features were calculated from the full resolution data and are herein collectively termed the "critical values." Table 2 and Figure 2 give a brief written and graphical description of the 22 critical values. Several of these values warrant additional clarification. The red edge (critical value 6) was calculated by finding the wavelength, between the red and near infrared regions of the spectrum, where the first derivative (slope) was at its maximum. The NDVI (Normalized Difference Vegetative Index) value was developed by Tucker (1979) and is a ratio of the difference between TM4 and TM3 (critical values 10 and 11) to the sum of TM4 and TM3  $((TM4 - TM3)/(TM4 + TM3))$ .

Critical values 13 through 18 (Table 2) represent feature extractions from the red absorption trough and green reflectance peak area. In the case of the red absorption trough, a continuum is created that connects the highest point in the green region to a point on the NIR (near infrared) shoulder where this line has the steepest slope. For the green reflectance peak, a continuum is defined that connects the lowest point on the blue trough with the lowest point on the red trough. In both cases the continuum is divided into the original spectrum to normalize the absorption and reflectance bands to a common reference. The asymmetry of the respective features is defined as the sum of the reflectance values to the right of the red minimum (or green maximum) divided by the sum of the reflectance values to the left. This method of feature extraction was adapted and expanded from a study by Singhroy and Kruse (1991).

The 41-channel data set is composed entirely of percent reflection values. All of this information is, therefore, brightness related. The 22 critical values also contain brightness information in specific regions, but in addition, contain significant positional and shape information.

TABLE 2. DESCRIPTION OF CRITICAL VALUES CALCULATED FROM 205-CHANNEL SE-590 PERCENT REFLECTANCE SPECTRAL DATA.

1. BluBrt	Percent reflectance of blue absorption trough
2. GrnWv	Wavelength position of (micrometres) green reflectance maximum
3. GrnBrt	Percent reflectance of green reflectance maximum
4. RedWv	Wavelength position of (micrometres) red absorption trough
5. RedBrt	Percent reflectance of red absorption trough
6. RdEdWv	Wavelength position of inflection point on "red edge"
7. RdEdBrt	Percent reflectance at inflection point on "red edge"
8. TM1	Band weighted average of percent reflectance in Landsat Thematic Mapper band 1 region (0.43-0.55 $\mu\text{m}$ )
9. TM2	Band weighted average of percent reflectance in Landsat Thematic Mapper band 2 region (0.51-0.65 $\mu\text{m}$ )
10. TM3	Band weighted average of percent reflectance in Landsat Thematic Mapper band 3 region (0.60-0.74 $\mu\text{m}$ ).
11. TM4	Band weighted average of percent reflectance in Landsat Thematic Mapper band 4 region (0.74-0.93 $\mu\text{m}$ ).
12. NDVI	Normalized Difference Vegetation Index ((TM4-TM3)/(TM4 + TM3))
13. RTDepth	Depth of red trough after removal of green maximum to NIR shoulder continuum.
14. RTAsym	Asymmetry measure of continuum-removed red trough.
15. RTFWHM	Full width at half depth of continuum-removed red trough.
16. GPHght	Height of green peak after removal of blue trough to red trough continuum.
17. GPAsym	Asymmetry measure of continuum-removed green peak.
18. GPFWHM	Full width at half height of continuum-removed green peak.
19. MShld	Slope of line from green peak to high point on NIR shoulder.
20. MLsSq	Slope of best fit (least squares) line through green and red wavelength regions (0.51-0.71 $\mu\text{m}$ ).
21. RTWv	Wavelength position of minimum in red region for continuum-removed curve.
22. GPWv	Wavelength position of maximum in green region for continuum-removed curve.

## Correlation Analysis

The statistical analysis of the spectral values was designed to show their relationship to the oil field's/area's boundaries and production trend. Three numerical parameters were defined and measurements made for each of the samples for incorporation into data matrices. The first parameter is designated Oil Index (OI), and indicates the location of the sample site with respect to surface or subsurface hydrocarbons. Another parameter is termed Distance to Center (DC) and is defined as the straight-line distance between the sample locality and the center or structural apex of the field as mapped on the dominant production formation. The third parameter is called Distance to Axis (DA) and is defined as the shortest straight-line distance between the sample locality and the closest point on the structural axis of the field as mapped on the dominant productive formation.

At least six separate data matrices were compiled from each of the six areas studied. The six regular spectral data sets consisted of (1) black cloth 41-channel spectral values,

(2) clump 41-channel spectral values, (3) fiber optic 41-channel spectral values, (4) black cloth 22 critical values, (5) clump 22 critical values, and (6) fiber optic 22 critical values. The spectral data were combined with the three numerical parameters (OI, DC, DA) and four production parameters which are dummy variable columns (Barren, Edge, Productive, Seep/Tar) that indicate the absence or nature of underlying surface hydrocarbons present. Correlation matrices were calculated for each of the 30+ data sets to determine the statistical interrelationships that exist between reflectance spectra of sagebrush, measurement techniques (i.e., black cloth, clump, fiber optic), and hydrocarbon occurrence.

## Results

### Correlation Analysis - 22 Critical Values

Although numerous significant correlations are found throughout the database, the most reliable relationships are those found to be consistent by all three data sets (i.e., BC, CL, and FO) and repeated in several fields. Table 3 divides these correlations on the basis of sample area and "criteria levels." Criteria Level 1 designates relationships that are significant at the 95 percent confidence level, or higher, in all three data sets, and in the same direction (+ or -) for individual fields. Criteria Level 2 designates relationships that are significant at the 95 percent confidence level, or higher, in two out of three data sets (i.e., black cloth, clump, fiber optic) for the individual fields. For Criteria Level 2 relationships, the lowest correlation, although not significant at the 95 percent level, must be in the same direction as the other two. Eight of the original 22 critical values appear to be important in the detection of near-surface hydrocarbons and

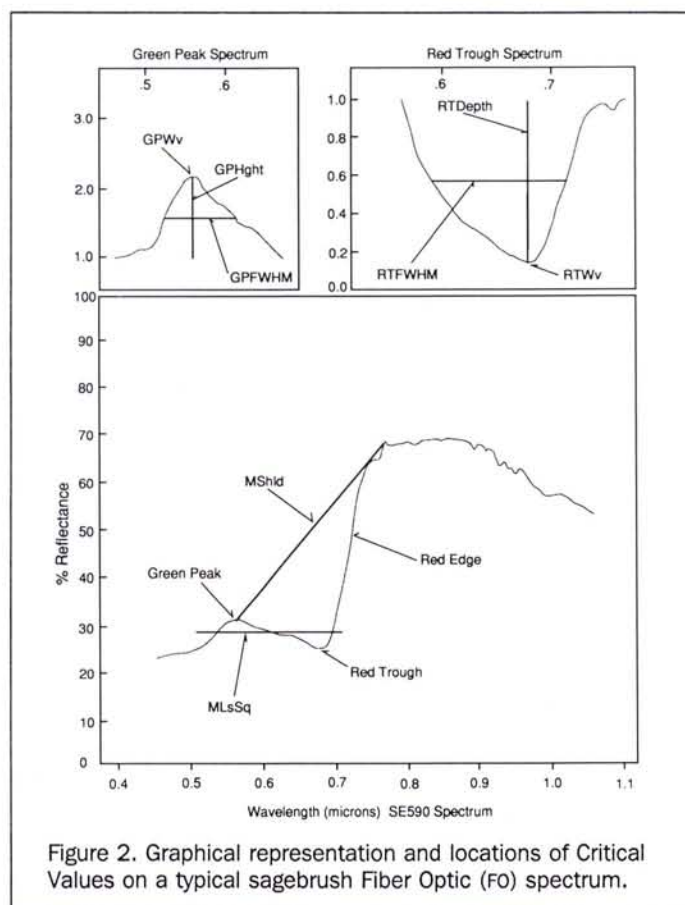


Figure 2. Graphical representation and locations of Critical Values on a typical sagebrush Fiber Optic (FO) spectrum.

TABLE 3. CLASSIFICATION AND COMPARISON OF SIGNIFICANT CORRELATIONS CALCULATED BETWEEN THE 22 CRITICAL VALUES AND THE DISTANCE AND HYDROCARBON PARAMETERS.

Criteria Level 1 All 3 measurement types @ 95% significant	Criteria Level 2 2 of 3 measurement types 95% significant and 3rd in same direction
<b>Trapper Canyon Tar Sand Deposit</b>	
Seep/Tar vs. GrnWv (-)	Seep/Tar vs. GPFWHM (-)
Seep/Tar vs. RedWv (-)	Seep/Tar vs. RTWv (-)
Seep/Tar vs. RTFWHM (+)	
<b>Bonanza Oil Field</b>	
Seep/Tar vs. GrnWv (-)	Seep/Tar vs. GPWv (-)
Seep/Tar vs. RedWv (-)	Seep/Tar vs. NDVI (-)
Seep/Tar vs. RdEdWv (-)	
Seep/Tar vs. RTWv (-)	
Dist A vs. NDVI (+)	
<b>Little Buffalo Basin Oil Field</b>	
0	Edge vs. RTDepth (+)
<b>Little Buffalo Basin Oil Field (east dome)</b>	
0	Barren vs. GrnWv (+)
	OI vs. GrnWv (-)
	Dist A vs. GrnWv (+)
	Dist A vs. GPWv (+)
<b>Enigma Oil Field</b>	
0	0
<b>Cody Base Area</b>	
0	0

41-channel reflectance data and surface or subsurface hydrocarbons.

Table 3 shows that most of the significant and repeatable correlation coefficients are found in the Trapper Canyon and Bonanza data sets, and involve relationships with the Seep/Tar sample sites. The GrnWv and RedWv positional measurements are the most undeviating. At both the Trapper Canyon and Bonanza areas the green peak (GrnWv) and red trough (RedWv) positions shift to lower wavelengths (blue shift) at Seep/Tar locations. These are the only two measures found consistent and significant in all of the six data sets for Trapper Canyon and Bonanza. The RTWv measure also shifts toward shorter wavelengths at Seep/Tar sites in the two fields, but this relationship is significant (>95 percent confidence level) in only five of the six possible data sets. The RdEdWv and GPWv measures show a blue shift at Seep/Tar sites but are only significant at Bonanza.

Two feature extraction measures are found to have significant correlations at the Trapper Canyon Tar Sand Deposit. The width of the normalized red trough (RTFWHM) increases and the width of the normalized green peak (GPFWHM) decreases for Seep/Tar reflectance spectra. As previously noted, both the green peak and red trough shift to lower wavelengths, but the red Edge (RdEdWv) does not shift systematically at Trapper Canyon. The shifting of these two wavelength positions and the respective stability of the red Edge position results in an expansion of the red trough and a compression of the green peak. Therefore, the shifting of the green and red inflection point pair (GrnWv and RedWv) and the change in the respective curves (GPFWHM and RTFWHM) can be directly related to each other. In contrast, because the red Edge position (RdEdWv) at Bonanza shifts in concert with the green and red inflection points, no systematic changes in the green peak or red trough widths are found. A consistent blue shift of the green peak and red trough can be measured in the Seep/Tar parameter at Trapper Canyon and Bonanza. This shift, with respect to the average of the other three parameters, ranges from 0.00168 to 0.00693 micrometres (Figures 3 and 4).

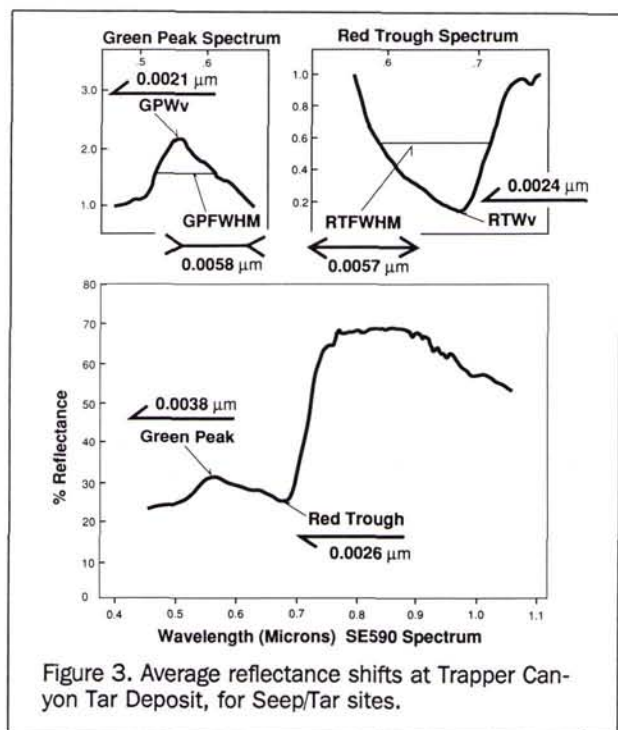


Figure 3. Average reflectance shifts at Trapper Canyon Tar Deposit, for Seep/Tar sites.

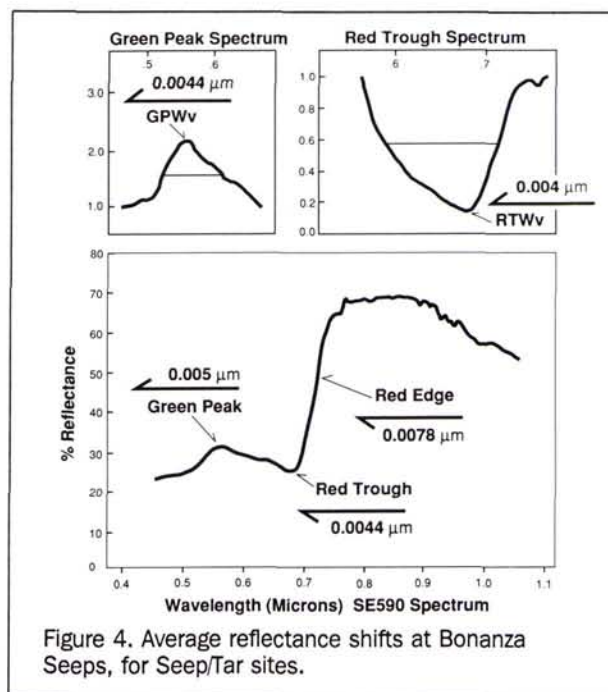


Figure 4. Average reflectance shifts at Bonanza Seeps, for Seep/Tar sites.

vegetational stress. These values include five wavelength positional measures (GrnWv, RedWv, RTWv, RdEdWv, and GPWv), two feature extraction measures (RTFWHM and GPFWHM), and one reflectance ratio measure (NDVI). No consistent and significant relationships are found between the

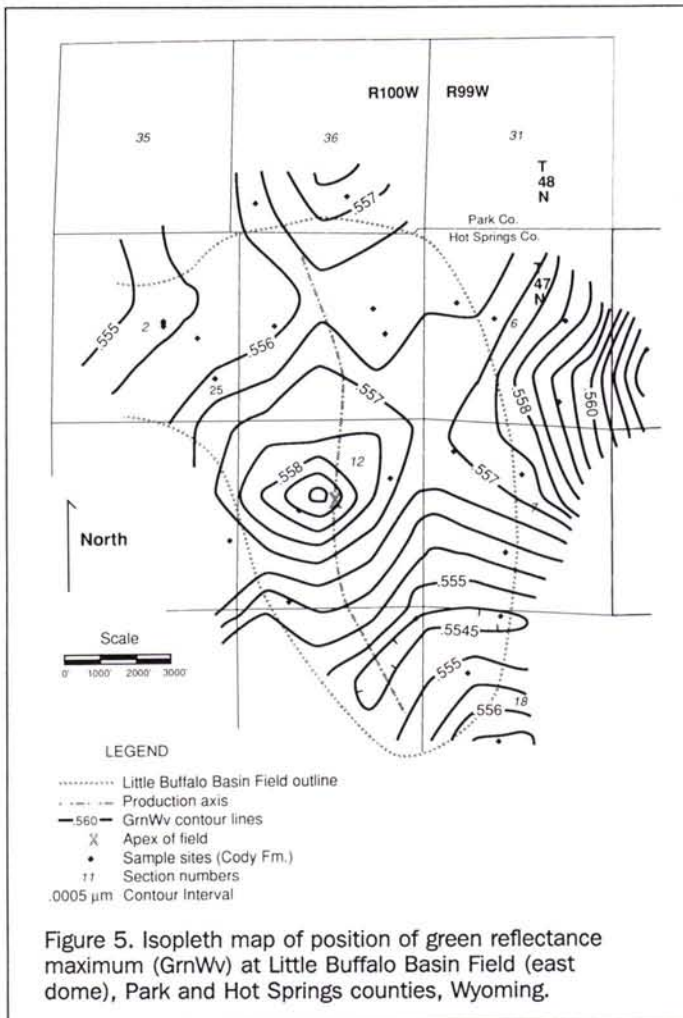


Figure 5. Isopleth map of position of green reflectance maximum (GrnWv) at Little Buffalo Basin Field (east dome), Park and Hot Springs counties, Wyoming.

The only reflectance intensity related measure that falls within either Criteria level is NDVI. This, though, is a ratio and gives a measure of the internal relationship between TM bands 3 and 4, and is not dependent on the absolute intensity of the overall spectrum. NDVI is shown to decrease at the Seep/Tar site and increase as the distance to the axis increases at the Bonanza area. Taken together, these two correlations (NDVI versus Seep/Tar and NDVI versus Dist A) are compatible.

Outside of the Trapper Canyon and Bonanza areas, no correlations are found that meet the first Criteria Level. Several correlations, though, are found in the Little Buffalo Basin data set that fall into the second Criteria Level. Over the entire Little Buffalo Basin area (i.e., both east and west domes), an increase in the normalized red trough depth (RTDepth) is found at the Edge sites. However, when only the east dome of Little Buffalo Basin is analyzed, the RTDepth relationship disappears and several somewhat more significant correlations are found involving the position of the green peak. The green peak (GrnWv) correlates with the Barren, OI, and Dist A parameters, and the normalized green peak (GPWv) correlates with Dist A. This set of four relationships is internally consistent and points to a shift in the green peak toward longer wavelengths as the distance to the axis increases. This set of relationships is also consistent with those found at Trapper Canyon and Bonanza.

Figure 5 is an isopleth map of the GrnWv values at the

east dome of Little Buffalo Basin. The contour pattern is somewhat variable but reveals that, in general, GrnWv values increase going away from the oil field. In section 12, though, two GrnWv values directly over the apex of the oil field form a small contour high area. These values for GrnWv are not as high as the values to the east in sections 6 and 7.

Although the relationship between the GrnWv values and the underlying oil and gas field is not overwhelming, the tendency toward a blue shift in GrnWv values is found in sagebrush over the productive (and Edge) areas. This relationship appears to be driven by the unique values at Barren sites rather than the Productive values. The Productive category at Little Buffalo Basin (east dome) displays a small but consistent blue shift of the green peak (Figure 6).

A total of 17 relationships are found within the data sets of the six samples areas that fall into one of the two Criteria levels. Taken as a whole, all of the correlations except three indicate a blue shift in position for the green and red inflection points as the presence of hydrocarbons increase.

### Comparison of the Eight Critical Values

In order to determine the actual magnitudes of change present within these eight critical values, the values were averaged together according to area data set (i.e., black cloth, clump, or fiber optic), and category (i.e., Barren, Edge, Productive, or Seep/Tar) (Table 4). It is apparent that the Seep/Tar category at Trapper Canyon and Bonanza displays the most distinct and orderly arrangement in respect to the other three categories. This would have been predicted by the preceding correlation analysis.

### Principal Component Analysis

The correlation analysis has shown that eight of the original 22 critical values are relevant to this study. Of these eight values, seven (GrnWv, RedWv, GPWv, RTWv, RdEdWv, GPFWHM, and RTFWHM) are closely related and, in general, vary together. In an effort to exploit these redundant data and to reduce the information into two or three dimensions

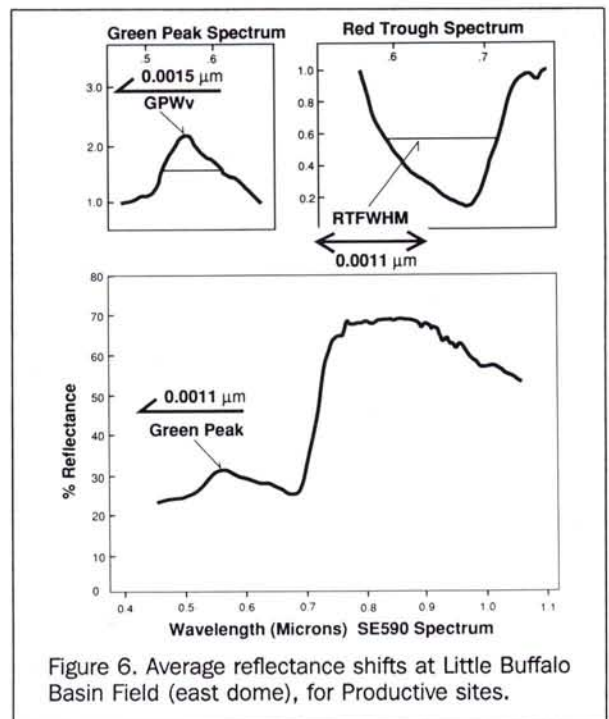


Figure 6. Average reflectance shifts at Little Buffalo Basin Field (east dome), for Productive sites.

TABLE 4. MAGNITUDE OF BLUE SHIFT AT THE SIX AREAS OF INTEREST

	GrnWv	RedWv	RdEdWv	RTWv	GPWv
<b>Trapper Canyon Tar Sand Deposit</b>					
Black Cloth	0.0069	0.0043	0.0010	0.0052	0.0053
Clump	0.0026	0.0017	0.0003	0.0023	0.0002
Fiber Optic	0.0021	0.0017	-0.0015	-0.0001	0.0007
<b>Bonanza Oil Field</b>					
Black Cloth	0.0048	0.0056	0.0113	0.0037	0.0031
Clump	0.0057	0.0026	0.0057	0.0042	0.0052
Fiber Optic	0.0051	0.0050	0.0065	0.0053	0.0038
<b>Little Buffalo Basin Oil Field</b>					
Black Cloth	0.0008	-0.0006	0.0013	0.0001	0.0008
Clump	0.0012	0.0007	-0.0001	-0.0001	0.0020
Fiber Optic	-0.0007	-0.0006	-0.0015	-0.0006	-0.0004
<b>Little Buffalo Basin Oil Field (east dome)</b>					
Black Cloth	0.0018	-0.0009	0.0005	0.0008	0.0014
Clump	0.0007	0.0010	0.0006	0.0002	0.0024
Fiber Optic	0.0007	0.0001	-0.0009	0.0001	0.0006
<b>Enigma Oil Field</b>					
Black Cloth	-0.0010	-0.0003	-0.0021	-0.0005	-0.0007
Clump	-0.0013	0.0007	-0.0019	0.0006	-0.0007
Fiber Optic	0.0004	0.0001	-0.0009	-0.0004	0.0002
<b>Cody Base Area</b>					
Black Cloth	-0.0007	0.0005	0.0047	0.0026	0.0007
Clump	-0.0007	-0.0005	-0.0020	0.0010	-0.0007
Fiber Optic	0.0010	0.0019	0.0010	0.0022	0.0010

\*\* Blue shift at Trapper Canyon and Bonanza = ((Barren + Edge + Productive)/3 - Seep/tar)

\*\* Blue shift at other areas = ((Barren + Edge)/2 - Productive)

rather than eight, a principal component (PC) analysis was performed.

A set of correlation analyses using the eight new PC axes as measures versus the distance and hydrocarbon parameters show that the most significant (*i.e.*, highest) and consistent correlations are found at Bonanza and Trapper Canyon involving the Seep/Tar parameter. In all six data sets for these two areas, the Seep/Tar parameter has a negative correlation with PC1. Five of these relationships are significant at the 95 percent Confidence level or higher (four fall within the 99 percent range). Although it is difficult to determine exactly what characteristics from the original eight critical values are being represented by PC1, the first principal component is usually dominated by highly correlated features. Within these data sets the effects of the blue shift must be largely responsible for the strengths and direction of the calculated PC1 versus Seep/Tar relationships.

### Data Reduction and Principal Component Plotting

Analysis of the original spectra has progressed through a series of steps designed to distill the information into a small but meaningful package. The original spectral readings for each data set (*i.e.*, BC, CL, FO) consisted of 756 numbers at each sample site (*i.e.*, readings of three individual sages). These three measurements were averaged into a site mean, ratioed against a Fiberfrax standard, and trimmed to produce a 205-channel reflectance spectrum at each site. Each 205-channel spectrum was simultaneously reduced into separate 41-band spectral and 22-band critical value files for analysis. Eight of the critical values were extracted and projected onto a new hierarchical coordinate system using a principal component analysis. Correlation analyses of the eight principal component coordinates identified the ones most highly correlated with the hydrocarbon and/or distance parameters.

The initial set of 756 values taken at each sample site has been condensed into a handful of values which may be used in an effort to discriminate sites into particular category types (*i.e.*, Barren, Edge, Productive, and Seep/Tar).

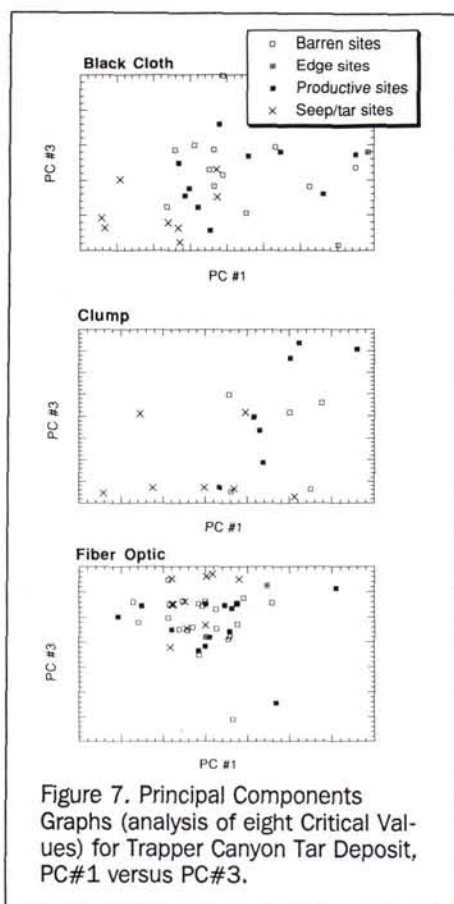
Figures 7 through 9 are graphs for three areas in which the categories are denoted by different symbols and plotted according to calculated PC values. The particular pair of PCs used were determined in part by the preceding correlation analysis, and are intended to show the maximum distinction possible between the categories.

The most consistent and widest distinctions are found within the Bonanza and Trapper Canyon information. At both of these areas, especially Bonanza, the Seep/Tar sample points are generally found separate from the other three categories. The FO PC plot from Bonanza exhibits a particularly tight and distinct cluster of Seep/Tar sample sites. In the BC and CL Bonanza PC plots, some co-mingling exists, but the Seep/Tar sample points are found toward a particular corner, indicating that separation is found in each of the two PCs plotted. On the other hand, all of the separations for the FO PC plots are found in the first principal component.

Considerably more mixing occurs in the Trapper Canyon PC plots between the Seep/Tar and other sample points. Within two data sets, (BC and CL) the Seep/Tar points tend toward the lower left-hand corner, indicating low values and separation on both of the PC axes. As opposed to the excellent discrimination for Seep/Tar sites exhibited in the Bonanza FO plot, the poorest distinctiveness is found in the Trapper Canyon FO plot. No consistent discriminations are found at any of the six areas between the Barren, Edge, or Productive sample sites.

### Discussion

Several basic types of information have been gleaned and processed from the original spectra. These include reflectance



tance intensities, feature or shape measurements, and positional information.

McCoy *et al.* (1989), in a similar but more localized reflectance study, reported "a greater energy reflectance in the near infrared in oil producing areas" at the Blackburn Oil Field, Nevada. Reflectance intensities were evaluated in the present study using the 41-channel spectra as described previously. No consistent, statistically significant, relationships at any of the six areas were detected responding to the presence or absence of surface or subsurface hydrocarbons. Even in the extreme cases at Trapper Canyon and Bonanza, where visible hydrocarbons are at the surface, no reflectance intensity-related response could be detected. Although each of these studies was undertaken in widely separated geologic basins, and it is impossible at this point to assess this variation, the results of this study cannot support the conclusions reached by McCoy *et al.* (1989).

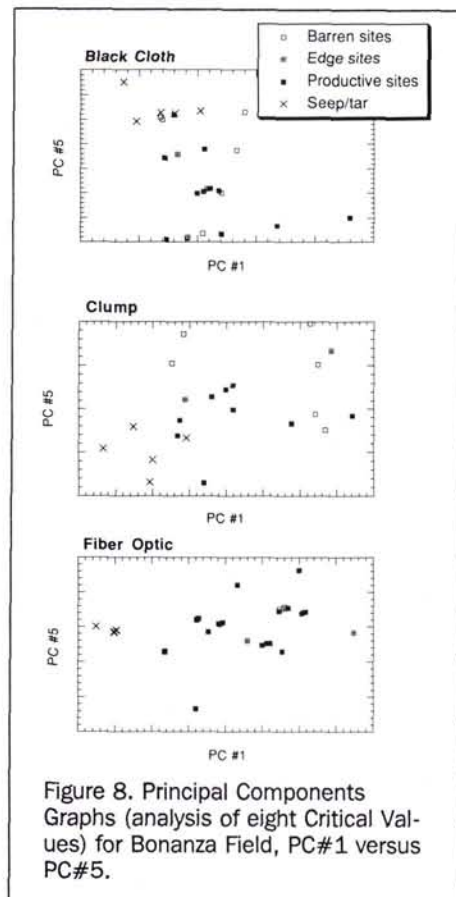
Selected shape measurements (feature extractions) and their relationships to the six areas were evaluated within the 22-channel Critical Value files. Singhroy and Kruse (1991) discussed using the depth (RTDepth) and width (RTFWHM) measurements of the normalized chlorophyll absorption band (red trough) in a study of ozone-stressed Ponderosa Pine and metal-stressed boreal forest species. They concluded that these two feature extractions (RTDepth and RTFWHM) are better indicators of metal stress due to a greater magnitude shift in these parameters than in positional shifts. A systematic change in the red trough width (RTFWHM) was observed only in the Trapper Canyon data (Figure 3), with no corresponding shift detected in the red trough depth (RTDepth). This shift in the RTFWHM is no more significant than other shifts observed in several positional measure-

ments. In contrast to the conclusion reached by Singhroy and Kruse (1991) in their ozone and metal stress-related study, positional data appear to be the measurement types most directly applicable to hydrocarbon presence.

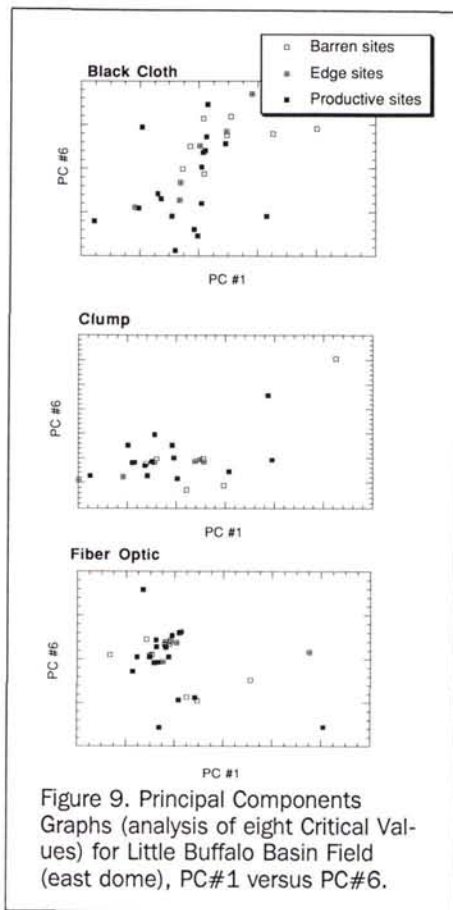
Throughout the process of analysis and data reduction, the ultimate goal has been to define and extract relevant data and apply it toward the detection of surface and, ultimately, subsurface hydrocarbons. At the extreme Seep/Tar sites in the Trapper Canyon and Bonanza areas, significant distinctions can be made using eight of the original 22 Critical Values. The other 15 Critical Values are not detectably affected by the presence of hydrocarbons. The discrimination generated by the use of these selected eight Critical Values only serves to separate the Seep/Tar sites from the other three. At Trapper Canyon and Bonanza, no distinctions can be made between the Barren, Edge, and Productive sites. In the other four areas examined, only at Little Buffalo Basin is there any hint of category discrimination. At the east dome of the Little Buffalo Basin, a small but statistically significant separation is found between the Barren category and the other two categories when analyzing for GrnWv. Several of the other eight critical values display a small (and consistent) but not statistically significant separation between the Barren category and the other two categories at the east dome of the Little Buffalo Basin Oil Field.

## Conclusions

- There are no consistent and significant correlations between the 41-channel spectral data and any distance or hydrocarbon parameters. Although significant correlations are found within the 41-channel spectral information, for some individ-







ual fields, they are not found to be consistent throughout all three data sets (BC, CL, FO) at any given area.

- Of the three data sets (BC, CL, FO) analyzed, no one measurement method is determined to be best. The Clump (CL) method though, appears to be a good compromise and allows for the most efficient data collection.
- A blue shift (shift to shorter wavelengths) of the green peak (GrnWv) and red trough (RedWv) are the most consistent and best indicators of the presence of surface and near-surface hydrocarbons. At both Trapper Canyon and Bonanza the GrnWv and RedWv shift from 0.0017 to 0.0069 micrometres toward shorter wavelengths in all three data sets (BC, CL, FO). The normalized green peak (GPWv) and red trough (RTWv) positions were less significant indicators, but still important.
- The behavior of the red edge inflection position (RdEdWv) may indicate the type of hydrocarbons present. The presence of light hydrocarbons and hydrocarbon gases at the Bonanza Seeps appears to have resulted in a significant (0.0113 to 0.0065 micrometres) blue shift in the red edge inflection point (RdEdWv) in all three data sets, in contrast to the Trapper Canyon Tar Sand area where only heavy hydrocarbons are present, and no shift in the red edge is detected.
- When all three of the visible region's positional measurements (GrnWv, RedWv, RdEdWv) shift together (as at Bonanza), no systematic changes were detected in the depth (RTDepth), width (RTFWHM), or asymmetry (RTAsym) of the normalized red trough. At Trapper Canyon, systematic changes in the RTFWHM and GPFWHM measures were found, resulting from a shift in the RdWv and GrnWv as the RdEdWv position remained constant.
- Out of the 22 original critical values, eight of these values tend to be measurably affected by surface hydrocarbons. These include five wavelength positional measures (GrnWv, RedWv, RTWv, RdEdWv, and GPWv), two feature extraction measures (RTFWHM and GPFWHM), and one reflectance ratio

measure (NDVI). The remaining 15 critical values, comprised mostly of reflectance intensity and feature extraction measures, are unaffected by the presence of hydrocarbons in the soil.

- A principal component analysis of the eight extracted critical values allows for a good discrimination between the Seep/Tar and the other three category types. Most of the distinctions brought out by the PC analysis result directly or indirectly from the blue shift of the visible region inflection points. Unfortunately, the PC analysis could not discriminate between all four category types (*i.e.*, Barren, Edge, Productive, and Seep/Tar) in question.
- Within the Bighorn Basin of Wyoming, spectral reflectance data from sagebrush are useful as a hydrocarbon indicator only in areas of visible occurrence or perhaps in areas of profuse (but not visible) vertical seepage.

## References

- Birnie, R.W., and J.R. Francica, 1981. Remote Detection of Geobotanical Anomalies Related to Porphyry Copper Mineralization, *Economic Geology*, 76:637-647.
- Crawford, M.F., 1991. Cement and Velma Oil Fields, *Remote Sensing Techniques Applied to Structural Geology and Oil Exploration in South Central Oklahoma*, AAPG Convention, Dallas, Texas.
- Dalziel, M.C., and T.J. Donovan, 1980. *Biogeochemical Evidence for Subsurface Hydrocarbon Occurrence, Recluse Oil Field, Wyoming, Preliminary Results*, U.S. Dept. Interior, Geological Survey Circ. 837, 11 p.
- Donovan, T.J., 1974. Petroleum microseepage at Cement, Oklahoma: evidence and mechanism, *AAPG Bulletin*, 58:429-446.
- Fox, J.E., and G.L. Dolton, 1989. *Petroleum Geology of the Wind River and Bighorn Basins, Wyoming and Montana*, USGS Open-File Report 87-450P, 41 p.
- Goetz, A.F.H., B.N. Rock, and L.C. Rowan, 1983. Remote sensing for exploration - an overview, *Economic Geology and the Bulletin of the Society of Economic Geologists*, 78(4):573-590.
- Klusman, R.W., M.A. Saeed, and M.A. Abu-Ali, 1992. The potential use of biogeochemistry in the detection of petroleum microseepage, *AAPG Bulletin*, 76:851-863.
- Kvale, E.P., 1986. *Paleoenvironments and Tectonic Significance of the Upper Jurassic Morrison/Lower Cretaceous Cloverly Formations, Bighorn Basin, Wyoming*, Unpublished Ph.D. thesis, Iowa State University.
- Lang, H.R., W.H. Alderman, and F.F. Sabins, Jr., 1984. *Patrick Draw, Wyoming, Petroleum Test Case Report: The Joint NASA/Geosat Test Case Project - Final Report*, section 11, pp. 11-i - 11-112.
- Malhotra, R.V., 1988. *A Field Spectrometer and Landsat TM Study of Surface Alteration Due to Hydrocarbon Seepage: Sheep Mountain Anticline, Bighorn Basin, Wyoming*, Unpublished master's thesis, Dartmouth College, 127 p.
- McCoy, R.M., and L.H. Wullstein, 1988. Mapping iron and manganese concentrations in sagebrush over the Blackburn oil field, Nevada, *Proceedings of the Sixth Thematic Conference on Remote Sensing in Exploration Geology*, Houston, Texas, pp. 523-528.
- McCoy, R.M., L.F. Scott, and P.J. Hardin, 1989. The spectral response of sagebrush in areas of hydrocarbon production, *7th Thematic Conference on Remote Sensing for Exploration Geology*, Calgary, Alberta, Canada, 6 p.
- Mitchell, C.D., Jr., 1988. *Detection of Vegetation Stress Related to Hydrocarbon Microseepage at the Velma Oilfield, Oklahoma Using Field Spectoradiometer, Geochemical and Landsat Thematic Mapper Data*, Unpublished master's thesis, University of Texas at Dallas, 225 p.
- Oehler, D.Z., and B.K. Sternberg, 1984. Seepage-induced anomalies, "false" anomalies, and implications for electrical prospecting, *AAPG Bulletin*, 68:1121-1145.

- Segal, D.B., and I.S. Merin, 1989, Successful use of Landsat Thematic Mapper data from mapping hydrocarbon microseepage-induced mineralogic alteration, Lisbon Valley, Utah, *Photogrammetric Engineering & Remote Sensing*, 55(8):1137-1145.
- Singhroy, V.H., and F.A. Kruse, 1991, Detection of metal stress in

Boreal Forest species using the 0.67  $\mu\text{m}$  chlorophyll absorption band. Presented at the Eighth Thematic Conference on Geologic Remote Sensing, Exploration, Engineering, and Environment, Denver, Colorado, 29 April - 2 May 1991.

## FORTHCOMING ARTICLES

- Kirk F. Adkins and Carolyn J. Merry, Accuracy Assessment of Elevation Data Sets Using the Global Positioning System.
- Robert J. Andres and William I. Rose, Description of Thermal Anomalies on Two Active Guatemalan Volcanoes Using Landsat Thematic Mapper Imagery.
- Peter August, Joanne Michaud, Charles LaBash, and Christopher Smith, GPS for Environmental Applications: Accuracy and Precision of Locational Data.
- William L. Baker, Jimmie J. Honaker, and Peter J. Weisberg, Using Aerial Photography and GIS to Map the Forest-Tundra Ecotone in Rocky Mountain National Park, Colorado, for Global Change Research.
- E. Ben-Dor, F. A. Kruse, A. B. Lefkoff, and A. Banin, Comparison of Three Calibration Techniques for Utilization of GER 63-Channel Aircraft Scanner Data of Makhtesh Ramon, Negev, Israel.
- David W. Bolgrien, Nick G. Granin, and Leo A. Levin, Surface Temperature Dynamics of Lake Baikal Observed from AVHRR Images.
- Paul V. Bolstad and Timothy Stowe, An Evaluation of DEM Accuracy: Elevation, Slope, and Aspect.
- B. Brisco and R. J. Brown, Multi-Date SAR/TM Synergism for Crop Classification in Western Canada.
- Daniel G. Brown and Thaddeus J. Bara, Recognition and Reduction of Systematic Error in Elevation and Derivative Surfaces from 7½-Minute DEMs.
- Duane C. Brown, New Developments in Photogeodesy.
- Keith C. Clarke, James A. Brass, and Phillip J. Riggan, A Cellular Automation Model of Wildfire Propagation and Extinction.
- Marco D'Errico, Antonio Moccia, and Sergio Vetrella, High-Frequency Observation of Natural Disasters by SAR Interferometry.
- C. Conese, M. A. Gilabert, F. Maselli, and L. Bottai, Topographic Normalization of TM Scenes through the Use of an Atmospheric Correction Method and Digital Terrain Models.
- Liping Di and Donald C. Rundquist, A One-Step Algorithm for Correction and Calibration of AVHRR Level 1b Data.
- Mary E. Dillworth, Jerry L. Whistler, and James W. Merchant, Measuring Landscape Structure Using Geographic and Geometric Windows.
- Melanie Dutkiewicz and Ian Cumming, Evaluation of the Effects of Encoding on SAR Data.
- Kathleen Edwards and Philip A. Davis, The Use of Intensity-Hue-Saturation Transformation for Producing Color Shaded-Relief Images.
- Max J. Egenhofer, Pre-Processing Queries with Spatial Constraints.
- L. Fent, R. J. Hall, and R. K. Nesby, Aerial Films for Forestry Inventory: Optimizing Film Parameters.
- Peter F. Fisher, Visualization of the Reliability in Classified Remotely Sensed Images.
- Giles M. Foody, Ordinal Level Classification of Sub-Pixel Tropical Forest Cover.
- Giles M. Foody, Mary B. McCulloch, and William B. Yates, Classification of Remotely Sensed Data by an Artificial Neural Network: Issues Related to Training Data Characteristics.
- Thomas D. Frank, Scott A. Tweddale, and David E. Knapp, Variability of At-Satellite Surface Reflectance from Landsat TM and NOAA AVHRR in Death Valley National Monument.
- Steven E. Franklin, Discrimination of Subalpine Forest Species and Canopy Density Using Digital CASI, SPOT PLA, and Landsat TM Data.
- Tung Fung and King-chong Chan, Spatial Composition of Spectral Classes: A Structural Approach for Image Analysis of Heterogeneous Land-Use and Land-Cover Types.
- Sucharita Gopal and Curtis Woodcock, Theory and Methods for Accuracy Assessment of Thematic Maps Using Fuzzy Sets.
- Armin Gruen and Thomas P. Kersten, Sequential Estimation in Robot Vision.
- Barry N. Haack and E. Terrance Slonecker, Merged Spaceborne Radar and Thematic Mapper Digital Data for Locating Villages in Sudan.
- Luheng Han and Donald C. Rundquist, The Response of both Surface Reflectance and the Underwater Light Field to Various Levels of Suspended Sediments: Preliminary Results.
- Kenneth C. Hardcastle, Photolineament Factor: A New Computer-Aided Method for Remotely Sensing the Degree to which Bedrock is Fractured.
- Perry J. Hardin, Parametric and Nearest-Neighbor Methods for Hybrid Classification: A Comparison of Pixel Assignment Accuracy.
- Perry J. Hardin and David G. Long, Discriminating between Tropical Vegetation Formations Using Reconstructed High-Resolution Seasat-A Scatterometer Data.
- L. W. Harding, Jr., E. C. Itsweire, and W. E. Esaias, Algorithm Development for Recovering Chlorophyll Concentrations in the Chesapeake Bay Using Aircraft Remote Sensing, 1989-1991.
- Paul M. Harris and Stephen J. Ventura, The Integration of Geographic Data with Remotely Sensed Imagery to Improve Classification in an Urban Area.
- Christian Heipke, State-of-the-Art of Digital Photogrammetric Workstations for Topographic Applications.
- Olaf Hellwich and Wolfgang Faig, Graph-Based Feature Matching Using Descriptive and Relational Parameters.
- E. Hierholzer, Calibration of a Video Rasterstereographic System.